Calculation of a HDR Blowdown Test Using a Substructure Method

D. Guilbaud, R.J. Gibert
C.E.A., CEN Saclay, DEMT, F-91191 Gif-sur-Yvette Cedex, France

Summary

This paper presents the results of a blowdown calculation and the comparison with a HDR test.

The calculations are made using a substructuration procedure, which is much cheaper than a 3D Finite Element analysis, because the specific geometric properties of the sub-structures (axisymmetrical shells - monodimensionnal pipes) can be used.

The comparison with the experimental data shows that the features of the pressure and displacement signals are well described and that the main modelisation problem is to know a good representation of the break zone ; a localized acoustical impedance tends to under-estimate the wave damping effects.

Introduction

During an hypothetical "loss of coolant accident"(LOCA) the pressure transient generated by the sudden break of a pressurized water reactor inlet pipe may induce large mechanical effects on the internal structure of the vessel.

Simplified methods could be employed for dealing with the early phase of the LOCA which is dominated by the acoustical propagation of pressure waves and their interaction with the structures. Indeed for a time of about 50 ms after the break the fluid is still mono-phasic almost everywhere in the circuit and the flow has just started at the broken pipe. At this step non linearities are expected to occur only at a few locations, for instance at the broken pipe outlet.

Here, a numerical method devoted to this early phase of the LOCA is used for studying the HDR blowdown (test V 29.2). Its main features are as follows :

- a subsystem procedure allows to deal with the strong 3D aspect of the problem,
- each subsystem is described by a modal basis consisting in a set of acoustical-mechanical coupled modes.

The main advantage of this method is to reduce significantly the cost of computation in comparison with the 3D explicit codes.

After a brief description of the modelisation, the computed results are compared with the HDR experimental data.

1. Summary of the substructuration procedure

The substructuration procedure has been already described in ref.[4] so we will only make here some recalls.

The complete system is divided into independant subsystems which are connected by some link forces (mechanical connection points) and some acoustical mass flow rates (fluid connection points).

The movement of each subsystem is described by its eigenmodes. The modal basis chosen corresponds to a free basis (neither forces nor acoustical sources exist at the connections).

Let us introduce α the modal contributions and the connection variables :

- for mechanical links :

  F_L : link forces developped by the substructure at the connection

  X_L : displacement of the mechanical connection point

- for fluid connections :

  D_L : fluctuating normal displacement of the fluid at the fluid connection areas

  P_L : fluctuating pressure at the fluid connections.

Each subsystem has to be in equilibrium under the external load and the connecting loads. After doing a modal projection the equations are the following :

$$\begin{bmatrix} K_G & B_X^T & 0 \\ B_X & 0 & 0 \\ 0 & 0 & 0 \end{bmatrix} \begin{bmatrix} \alpha \\ F_L \\ D_L \end{bmatrix} + \begin{bmatrix} M_G & 0 & B_\pi^T \\ 0 & 0 & 0 \\ B_\pi & 0 & A_{PM} \end{bmatrix} \begin{pmatrix} \ddot{\alpha} \\ \ddot{F}_L \\ \ddot{D}_L \end{pmatrix} = \begin{pmatrix} f_e + s_e \\ 0 \\ s_L \end{pmatrix} + \begin{pmatrix} 0 \\ X_L \\ P_L \end{pmatrix}$$

where K_G and M_G are the diagonal matrix of modal stiffnesses and masses

B_X matrix of coupling between the eigenmodes due to the mechanical links

B_π matrix of coupling between the eigenmodes due to the fluid connections

f_e external mechanical forces projected on the modal basis

s_e external acoustical sources " " " " "

A_{PM} mass matrix due to the fluid connections

s_L acoustical sources due to the fluid connections due to the external sources

A_{PM} and s_L may be computed from the quasi static responses at fluid connections to acoustical sources.

Now, the subsystems has to be joined together

- for mechanical links, we write :
  - . the equilibrium of forces
  - . the equality of displacements
- for fluid connections, we write :
  - . the continuity of the pressure
  - . the equality of normal displacements.

The modal contributions α , the link forces F_L and the fluid normal displacement D_L are obtained by solving this system. Then, the displacement and the pressure fields are computed from the modal basis.

II. Modelisation

a) Preliminary

The reactor is divided into two substructures. The vessel with the core barrel and the blowdown pipe. At the connections, the substructures are isolated by the boundary condition grad p.n = 0 (no mass flow rate through the connection area) so the symmetry of the vessel is preserved.

b) The pipe

In the pipe, only the movement of the fluid is represented by a set of acoustical modes of the closed pipe. The following criteria is used to truncate the modal basis : the lower eigen period must be about a quarter of the break opening time of the disk (1 ms). So the greater eigenfrequency is about 4000 Hz.

c) The vessel

The RPV and the core barrel are modelised with axisymmetrical shells by the code Aquamode. A set of acoustical-mechanical coupled modes have been computed and identified with the results of snapback tests. Here, only the modes the eigenfrequency of which is lower than 200 Hz are used in the computation because in the downcomer, the wave front is flatter than in the pipe as it can be seen in the experimental data. So the set of vessel modes is not complete enough to represent accurately the details of the pressure beneath the blowdown nozzle (see fig. 3). However, the computation goal is not to get back such details but the global shape of the time histories.

d) The fluid connections

Two fluids connections are employed

- the first one, to connect the downcomer and the inlet pipe
- the second one, to introduce an acoustical impedance which controls the wave reflexion on the two phase flow localized at the break.

e) Break representation

An acoustical impedance Z is used to simulate the wave reflexion on the two phase zone localized at the break. Moreover, this impedance allows to control the mass flow rate at the break. Now, it can be seen in the experimental data that the mass flow rate reaches a maximum value. So, a simple way to adjust this impedance is to choose the one which gets back the maximum.

f) Loading

The break of the disk creates :

- on one hand : an acoustical pressure source such as the pressure inside the pipe reaches the saturation pressure level,
- on other hand : a force F = PS (where P is the initial pressure in the vessel) due to the tension release in the pipe.

The loading time history is a simple step reached in one millisecond.

III. Discussion of the blowdown calculation results

The results of the computation with TRISTANA are drawn in dotted line, the experimental results in full line.

a) Pressure in the blowdown pipe

In fig. 1,one can see that the pressure wave travels with a velocity about 1000 m/s as prescribed in the code. In both experience and calculation the wave reflects on the downcomer at the same time.

However, the computation with TRISTANA does not get back the hard damping of the pressure waves in the pipe. In consequences, in the first 50 ms some oscillations of the not sufficiently damped waves can be seen for all the transducers localized in the neighbourhood of the blowdown nozzle.

b) Pressure in the downcomer

It is easy to verify that the pressure waves traveling in the axial direction in the thin downcomer region do not move at the 1000 m/s sonicvelocity of the bulk fluid but at approximately 450 m/s due to the interaction between the downcomer fluid, the core barrel and the pressure vessel wall.

The pressure decreases globaly in the downcomer, with a characteristic time associated with the resonance frequency of the Helmoltz system : vessel internal volume /blowdown tube.

When the decompression wave arrives in the downcomer the pressure starts to decrease. After about 30 ms, the pressure decrease stops momentarily as the result of the initial decompression wave from the blowdown nozzle, propagating down the annulus, reflecting as a compression wave from the lower plenum and traveling back up the downcomer to the blowdown nozzle.

After approximately 65 ms, the pressure begins to decrease again. This decrease is the result of the initial decompression wave reflecting as a further decompression wave at the top of the upper plenum and reversing its path back towards the blowdown nozzle.

c) Differential pressure across core barrel

The general shape of the computed pressure time history is in good agreement with the experimental data. When the pressure acting in the core barrel decreases, the core barrel starts moving towards the blowdown nozzle and the shell modes are excited. It is easy to verify that the large period of the measured signal corresponds to the period of the shell modes n = 2 and 3 (about 13 Hz).

d) Relative displacements of core barrel and RPV

The computation leads to underestimate the relative displacement. During the propagation of the decompression wave in the downcomer, the core barrel expands gradualy. After 30 ms, the core barrel starts to contract. Contraction of the barrel results from the decompression wave reaching the core region. In the same time, the core barrel begins to swing towards the blowdown nozzle.

e) Absolute displacement of the core barrel

For a large part, the movement of the core barrel is due to the tension release in the wall of the pipe which excites the first beam mode of the RPV. The period of the phenomenon is calculated accurately.

Conclusion

The model assumption that we have single phase, almost everywhere in the circuit seems to

work reasonably well for the period of about 50 ms. The discrepancies between measurement and calculation seems mainly due to a modelisation of the break zone. The constant acoustical impedance which represent this zone is a rough representation of the two phase flow phenomenon. An impedance versus time, and perharps of some other acoustical parameters in the pipe should have improved the results.

However, the coupling between fluid and structure seems to be well verified. The substructuration method used had required small computing time with regard to finite element code. Moreover,its implementation allows to measure better the relative weight of the physics phenomena which take place during the blowdown.

This method should be completed by 3D calculation in same localized zones, blowdown nozzle, break for knowing in details which happens in these areas.

References

[1] Jeanpierre, R.J., Gibert, Hoffman, Livolant. Fluid structure interaction. A general method used in the CEASEMT computer programs, SMIRT 5, Berlin 1979

[2] F. Axisa, R.J. Gibert. Non linear analysis of fluid structure coupled transients in piping systems. ASME PVP Conference, Orlando 1982, PVP63, p. 15

[3] Jeanpierre, Livolant. Experimental and theoretical methods for assessment of flow induced vibrations of nuclear internal structure. SMIRT 4, London 1977

[4] D. Guilbaud, F. Jeanpierre, R.J. Gibert. A substructure method to compute the 3D Fluid-structure interaction during blowdown, SMIRT 7, Chicago, 1983

[5] Wolf, Schumann, Scholl. Experiment and analytical results of coupled fluid structure interaction during blowdown of the HDR Vessel, SMIRT 7, Chicago, 1983

[6] Ludwig and Schumann. Fluid-structure analysis for the HDR blowdown and snapback experiments with FLUX Nuclear Engineering and Design 70 (1982) 321-333

[7] Chang, Santee, Mortensen, Gross, Belytschko. Loca hydroloads calculations with multi-dimensional nonlinear fluid-structure interaction, Nuclear Engineering and Design 70 (1982), 335-355

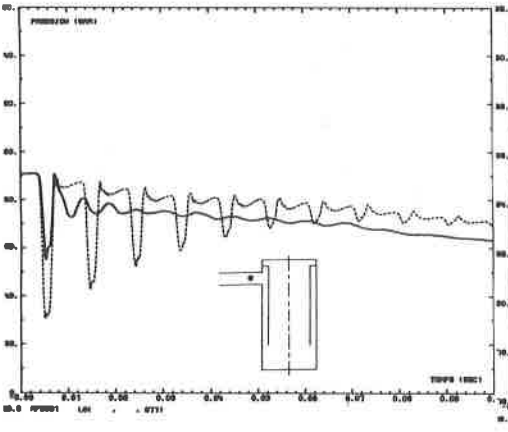

Figure 1 - Pressure in pipe

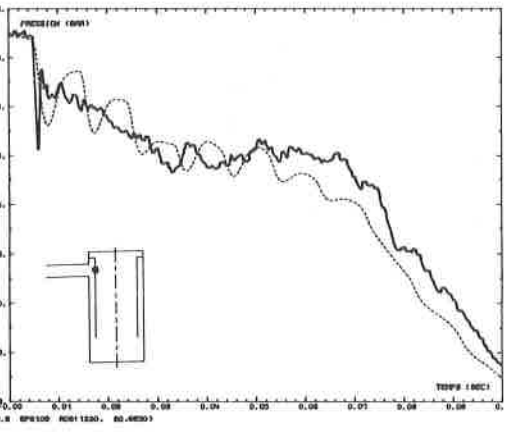

Figure 2 - Pressure in downcomer

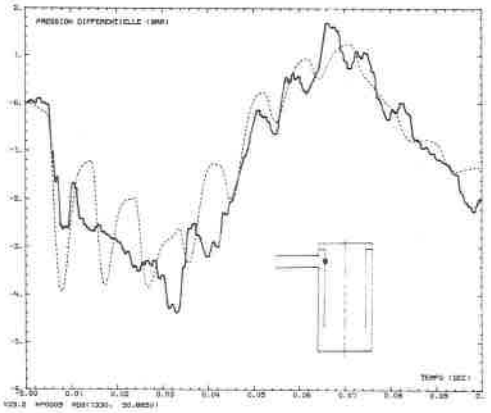

Fig. 3 - Pressure difference across core barrel

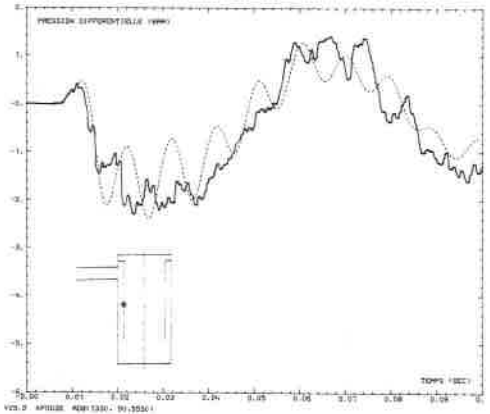

Fig. 4 - Pressure difference across core barrel

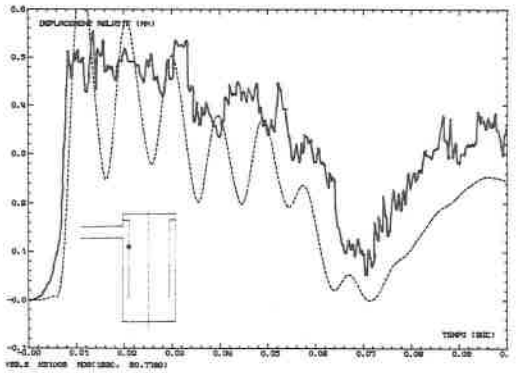

Fig. 5 - relative displacements of core barrel and RPV

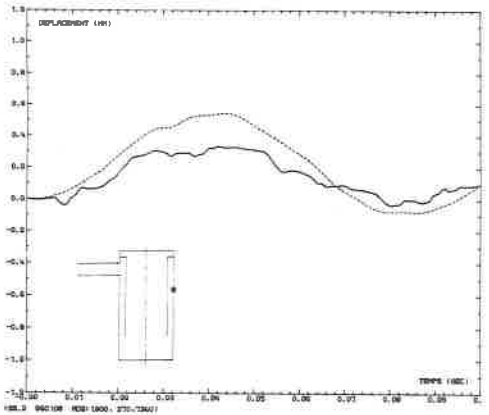

Fig. 6 - Absolute displacement of the RPV